Aggelos C. Iliopoulos*, Magdalini Tsolaki and Elias C. Aifantis

Tsallis statistics and neurodegenerative disorders

DOI 10.1515/jmbm-2016-0015

Abstract: In this paper, we perform statistical analysis of time series deriving from four neurodegenerative disorders, namely epilepsy, amyotrophic lateral sclerosis (ALS), Parkinson's disease (PD), Huntington's disease (HD). The time series are concerned with electroencephalograms (EEGs) of healthy and epileptic states, as well as gait dynamics (in particular stride intervals) of the ALS, PD and HDs. We study data concerning one subject for each neurodegenerative disorder and one healthy control. The analysis is based on Tsallis non-extensive statistical mechanics and in particular on the estimation of Tsallis q-triplet, namely $\{q_{\text{stat}}, q_{\text{sen}}, q_{\text{rel}}\}$. The deviation of Tsallis q-triplet from unity indicates non-Gaussian statistics and long-range dependencies for all time series considered. In addition, the results reveal the efficiency of Tsallis statistics in capturing differences in brain dynamics between healthy and epileptic states, as well as differences between ALS, PD, HDs from healthy control subjects. The results indicate that estimations of Tsallis q-indices could be used as possible biomarkers, along with others, for improving classification and prediction of epileptic seizures, as well as for studying the gait complex dynamics of various diseases providing new insights into severity, medications and fall risk, improving therapeutic interventions.

Keywords: EEGs; gait dynamics; neurodegenerative disorders; stride intervals; Tsallis q-triplet.

1 Introduction

Neurological disorders are major public health problems (e.g. around 50 million people suffer from epilepsy [1]). These disorders include diseases such as Alzheimer's disease and other dementias, brain cancer, degenerative nerve diseases, encephalitis, epilepsy, genetic brain disorders, head and brain malformations, hydrocephalus, stroke, Parkinson's disease (PD), multiple sclerosis, amyotrophic lateral sclerosis (ALS or Lou Gehrig's disease), Huntington's disease (HD) and others. They afflict the nervous system resulting in progressive nervous system dysfunction, associated with atrophy of the affected central or peripheral structures of the nervous system [1].

In this paper we are concerned with four neurodegenerative disorders, namely epilepsy, ALS, PD, HD: Epilepsy is a sudden paroxysmal and temporary disturbance of the brain's functioning during which the brain's nerve cells send out excessive electrical impulses causing episodes called seizures, which can be focal or generalized [2, 3]; ALS is generated by the destruction of motoneurons of the cerebral cortex, brain stem and spinal cord; HD is caused by the mutation of Huntington's gene; PD is caused by the malfunction of a neurotransmitter called dopamine that transports signals to the parts of the brain that control movement initiation and coordination ([4] and refs. therein).

Any information concerning the dynamics of neurodegenerative disorders can be very useful for decision-support tools for early detection and diagnosis, as well as the development of new biomarkers, etc. One way to provide such information is to study time series which can represent the neurodegenerative disorders' complex dynamics. Epilepsy can be studied using electroencephalograms (EEGs) which reflect the mean electrical activity of the brain, as measured with electrodes at different places on the head, yielding evidence regarding the underlying associated neural dynamics and the dynamical changes in the brain's electrical activity [5]. However, ALS, PD and HD affect the ability to move, creating serious gait abnormalities, characterized by loss or dysfunction of neurons in the motor, sensory, or cognitive systems [4]. Therefore, the analysis of temporal gait parameters (e.g. stride, stance or swing intervals) can be very useful for providing information of the mechanisms of movement disorders [6].

Indeed, various studies concerning EEGs and gait time series non-linear statistical analysis revealed the complex, non-linear and non-stationary nature of these signals. In particular, the spatiotemporal complexity of brain activity during health or seizure periods is characterized by various dynamical states (chaos, self-organized criticality, etc), while human gait also exhibits multifractal dynamics (e.g. [2, 7–12]). In this paper, we

***Corresponding author: Aggelos C. Iliopoulos,** Lab of Mechanics and Materials, Aristotle University, Thessaloniki 54124, Greece, e-mail: ailiopou@gmail.com
Magdalini Tsolaki: Department of Neurology, Aristotle University of Thessaloniki, Thessaloniki 54124, Greece
Elias C. Aifantis: Lab of Mechanics and Materials, Aristotle University, Thessaloniki 54124, Greece; Michigan Technological University Houghton MI 49931, USA; ITMO University, St. Petersburg 197101, Russia; and BUCEA, Beijing 100044, China

analyze EEGs and gait time series using statistical analysis based on Tsallis non-extensive statistical mechanics [13]. Recent studies showed the efficiency of Tsallis statistics in characterizing non-linear, non-Gaussian, multifractal statistics of complex signals such as the EEG recordings of patients with epilepsy [14–16]. In particular, we exploit the Tsallis q-triplet [17, 18], which can provide information not only for the statistical features of the time series but also for the rate of entropy production, the relaxation dynamics and non-equilibrium meta-stable stationary states of the neurodegenerative disease complex dynamics.

The paper is organized as follows: Section 2 presents the mathematical and theoretical framework concerning Tsallis non-extensive statistics. Section 3 contains the results of the statistical analysis of the experimental medical time series. Finally, Section 4 contains a summary of the present results, conclusions and a discussion on future directions.

2 Theoretical framework and methodology of data analysis

2.1 Tsallis non-extensive statistics

The dynamics of far-from-equilibrium non-linear complex systems are characterized by multifractality, long-range correlations and power law scaling. In order to efficiently describe such behavior, Tsallis developed a consistent and effective theoretical framework, named non-extensive statistical thermodynamics, which is based on a generalization of Boltzmann-Gibbs (BG) entropy.

In particular, the generalization of BG entropy is given by the relation [13]

$$S_q = k\frac{1-\sum_{i=1}^{W} p_i^q}{q-1} (q\in\mathbb{R},\ S_1 = S_{BG}), \tag{1}$$

where k is the Boltzmann's constant, W is a set of discrete states and q the degree of non-extensivity. The Tsallis entropy S_q measures the complexity of the system, while the parameter q measures the degree of non-extensivity of the system. For example, for two probabilistically independent systems A and B, Eq. (1) becomes

$$S_q(A+B) = S_q(A)+S_q(B)+(1-q)S_q(A)S_q(B). \tag{2}$$

The first part of Eq. (2) is additive while the second part is multiplicative, describing the long-range interactions between the two systems. For $q>1$ and $q<1$ Eq. (2) holds for sub-additivity and super-additivity, respectively [14]. When $q=1$, Eq. (2) corresponds to the entropy of the usual BG statistical mechanics, which is additive.

2.1.1 Tsallis q-triplet

Tsallis q-indices can describe features of the dynamics of the complex system in our study, such as sensitivity to the initial conditions, relaxation towards equilibrium of correlation functions, equilibrium distribution of energies, entropy production, etc. Here, we are interested in the indices $q_{sensitivity}$, $q_{relaxation}$, $q_{stationary}$, known also as the Tsallis q-triplet [17], which also constitutes the best empirical quantifier of non-extensivity. In the following we describe briefly the underlying mathematical framework concerning the Tsallis q-triplet (for an extensive review, see [19]):

2.1.1.1 Tsallis q-sensitivity index (q_{sen})

According to [20] the power law sensitivity to initial conditions at the edge of chaos provides a natural link between the entropic index q and the attractor's multifractal or singularity spectrum $f(a)$. Therefore, we can use the multifractal spectrum to determine the entropic index q_{sen}, which is given by

$$q_{sen} = 1-\frac{a_{max}a_{min}}{a_{max}-a_{min}}. \tag{3}$$

The a_{max}, a_{min} values correspond to the extremes of multifractal spectrum for which $f(a)=0$. The knowledge of the Tsallis q_{sen} index is very important since it can be used to calculate the sensitivity to initial conditions $\xi(t)$ and the q-generalized Lyapunov exponent $\lambda_{q_{sen}}$. In particular, in the non-extensive scenario $\xi(t)$ is given by

$$\xi(t) = [1+(1-q_{sen})\lambda_{q_{sen}} t]^{1/(1-q_{sen})}. \tag{4}$$

Then we can use the extension of Pesin's theorem to make the important connection between the loss of information measure, via entropy production [17]

$$K_{q_{ent}} \equiv \lim_{t\to\infty} \frac{S_{q_{ent}}}{t}. \tag{5}$$

and the sensitivity to initial conditions. This result can be expressed by the q-generalized Pesin-like identity $K_{q_{ent}} \equiv \lambda_{q_{sen}}$ with $q_{ent}=q_{sen}$.

We followed Pavlos's [19, and refs. therein] for the estimation of the multifractal spectrum $f(a)$ from an experimental time series. In particular, if the experimental time

series is denoted by $x(t_i)$, we define a new scalar stationary variable $\Delta x(t_i)$ denoting the small-scale differences

$$\Delta x(t)=x(t_i+\Delta t)-x(t_i), \tag{6}$$

where Δt is the sampling interval. Then, we assign an appropriate probability measure $d\mu$ to the time series, which should scale with the resolution length, equal to

$$d\mu(t)=\frac{\Delta x(t)}{T\langle X\rangle}dt, \tag{7}$$

where T is the total time length. The coarse-grained probability is given by

$$p_i(\tau)=\int_{\Lambda_i} d\mu(\mathrm{t})\approx \sum_{t_i\le t'\le t_i+\tau}\Delta\mu(t'), \tag{8}$$

where $\tau=2^n$ is the size of the segments Λ_i with i=1, 2, …, $N(\tau)$, and $N(\tau)$ is the number of segments necessary to "cover" the time series. Consequently, the estimation of the "mass" moment scaling takes place captured by the function $\Gamma(\bar{q}, \tau)$ according to

$$\Gamma(\bar{q}, \tau)=\sum_{\Lambda_i} p_i(\tau)^{\bar{q}}\approx(\tau)^{\gamma(\bar{q})}, \tag{9}$$

where the "mass" exponent $\gamma(\bar{q})=(\bar{q}\text{-}1)D_{\bar{q}}$ and $D_{\bar{q}}$ are the generalized (Renyi) dimensions given by

$$D_{\bar{q}}=\frac{1}{\bar{q}\text{-}1}\lim_{\tau\to 0}\frac{\log\sum p^{\bar{q}}}{\log\tau} \tag{10}$$

which are estimated by a non-linear regression algorithm. The Renyi dimensions can be connected with the fractal dimensions $f(a)$ through the Legendre transformation

$$a=\frac{d\gamma(\bar{q})}{d\bar{q}},\ \gamma(\bar{q})\overset{\min}{=}_{a}\bar{q}\alpha\text{-}f(\alpha) \tag{11}$$

from which the singularity or multifractal spectrum $f(a)$ is estimated.

2.1.1.2 Tsallis q-relaxation index (q_{rel})

The Tsallis q_{rel} index is related with the relaxation process of a macroscopic quantity O of a complex system. This process represents the system's exploration in its full dynamical space, searching for possible metastable stationary state(s). The relaxation process can be described by the quantity [21]

$$\Omega(t)\equiv\frac{\mathrm{O}(t)\text{-}\mathrm{O}(\infty)}{\mathrm{O}(0)\text{-}\mathrm{O}(\infty)}. \tag{12}$$

The differential equation which relates the relaxation process to the Tsallis q_{rel} entropic index is

$$\frac{d\Omega}{dt}=\text{-}\frac{1}{\tau_{q_{\mathrm{rel}}}}\Omega^{q_{\mathrm{rel}}}, \tag{13}$$

where $\tau_{q_{\mathrm{rel}}}$ is the relaxation time and yields a solution of

$$\Omega(t)=[1\text{-}(1\text{-}q)(t/\tau_{q_{\mathrm{rel}}})]^{1/(1\text{-}q)}. \tag{14}$$

As candidate observables $\Omega(t)$ for estimation of q_{rel}, one can use the autocorrelation function or the average auto-mutual information. Here we use the latter, due to its efficiency to capture non-linear-linear features in contrast with the autocorrelation function which accounts only for linear characteristics. In particular, the q_{rel} index is given by $q_{\mathrm{rel}}=(b\text{-}1)/b$, where b is the slope of the log-log plotting of auto-mutual information I_{KK_τ} given in [22] by the relation:

$$I=\sum_{x(t),x(t+\tau)} p(x(t), x(t+\tau))\log_2\frac{p(x(t), x(t+\tau))}{p(x(t))p(x(t+\tau))}, \tag{15}$$

Auto-mutual information provides information gained about one measurement of a time series from the measurement of another. If the two measurements are completely independent, the auto-mutual information, is zero.

2.1.1.3 Tsallis q-stationary (q_{stat})

This index is connected with heavy-tail distributions, named the Tsallis q-Gaussian distributions. The estimation of the Tsallis q index, referred to as stationary $q=q_{\mathrm{stat}}$, is related to the size of these distribution tails and can describe metastable stationary states of the system. The Tsallis q-Gaussian distribution [23] is given by:

$$G_q(\beta; x)=\frac{\sqrt{\beta}}{C_q}e_q^{\text{-}\beta x^2}, \tag{16}$$

where $e_q=[1+(1\text{-}q)x]^{1/(1\text{-}q)}$ is the q-exponential, β is a positive number and C_q is a normalization constant, namely $C_q=\int_{-\infty}^{\infty}e_q^{\text{-}x^2}dx$. Depending on the q- value, C_q has the following forms:

$$C_q=\frac{2\sqrt{\pi}\Gamma\left(\frac{1}{1\text{-}q}\right)}{(3\text{-}q)\sqrt{1\text{-}q}\,\Gamma\left(\frac{3\text{-}q}{2(1\text{-}q)}\right)},\ -\infty<q<1, \tag{17}$$

$$C_q=\sqrt{\pi},\ q=1, \tag{18}$$

$$C_q=\frac{\sqrt{\pi}\Gamma\left(\frac{3-q}{2(q-1)}\right)}{\sqrt{q-1}\Gamma\left(\frac{1}{q-1}\right)},\ 1<q<3, \tag{19}$$

For $q<1$, the support of $G_q(\beta; x)$ is compact since this density vanishes for $|x|>1/\sqrt{(1-q)\beta}$.

The Tsallis q entropic index can be estimated by using the probability density function (PDF) computed from the experimental data $X=\{x_t;\ t=1, 2, \ldots, N\}$. The statistical analysis is based on the algorithm described in [19, and refs. therein]. We construct the PDF of the input time series as follows: The interval {min(X), max(X)} range is subdivided into bins of width δs, centered at s_i so that we can assess the frequency with which the X-values will fall within each bin. The resultant histogram is properly normalized (the sum of all probabilities is equal to unity) and yields the stationary PDF $\{p(x_i)\}_{i=1}^{N}$. Thus, p_i is the probability of an X-value to fall into the ith-bin centered at x_i. For the estimation of q-value, we vary q within the interval {1, 3} with a step $\delta q=0.005$ and the best q-value corresponds to the best linear fit [maximum correlation coefficients (cc)] of the graph $\ln_q(p(x_i))$ vs. x_i^2, where the function $\ln_q(x)=\frac{x^{1-q}-1}{1-q}$ corresponds to the q-logarithm (inverse of the q-exponential). Then, with the obtained q-value=q_{stat}, we compute the q_{stat}-Gaussian given by the equation above

$$G_q(\beta; x)=\frac{\sqrt{\beta}}{C_q}e_q^{-\beta x^2} \tag{20}$$

for different β-values. After selecting the β-value, minimizing the quantity $\sum[G_{q_{stat}}(\beta; x_i)-p(x_i)]^2$, we compare the experimental distribution with the theoretical q-Gaussian and with the normal Gaussian PDFs, in a $\log[p(x_i)]$ vs. x_i graph.

3 Signal analysis from neurodegenerative disorders

In this section, we present results concerning the estimation of the Tsallis q-triplet in EEGs corresponding to healthy and epileptic seizure dynamics, as well as in time series concerning gait dynamics related to ALS, PD and HD. For the estimation of the Tsallis q-triplet a first difference filter was used in all time series, namely the original values were replaced by $\Delta x_t=x_t-x_{t-1}$.

3.1 Epilepsy

We analyzed an EEG time series of a person suffering from epilepsy. In particular, we used data from the database, http://physionet.org/pn6/chbmit/ [24, 25], collected at the Children's Hospital Boston, MA, USA which consisted of EEG recordings from pediatric subjects with intractable seizures. The subjects were monitored for up to several days following the withdrawal of anti-seizure medication in order to characterize their seizures and assess their candidacy for surgical intervention. As a first case, a 11-year-old female was chosen. The records were taken for a total of 1 h, while the seizure lasted for 40 s.

Two time series were analyzed, one contained one seizure episode, while the other did not. Figure 1A shows the whole EEG time series including an epileptic episode (denoted between red lines, x4 segment), while Figure 1B shows an EEG time series of the same patient in which no episode was recorded. As it can be seen in Figure 1A,B the time series including the seizure episode is more erratic and irregular than the one without. We estimated the Tsallis q-triplet for the epileptic episode (x4-segment in Figure 1A) and for the time series with no episode (Figure 1B).

The results concerning the two time series are shown in Figure 2 (for comparison we show results concerning the second half of the time series in Figure 1B, but it must be noted that the results for the first half are very similar).

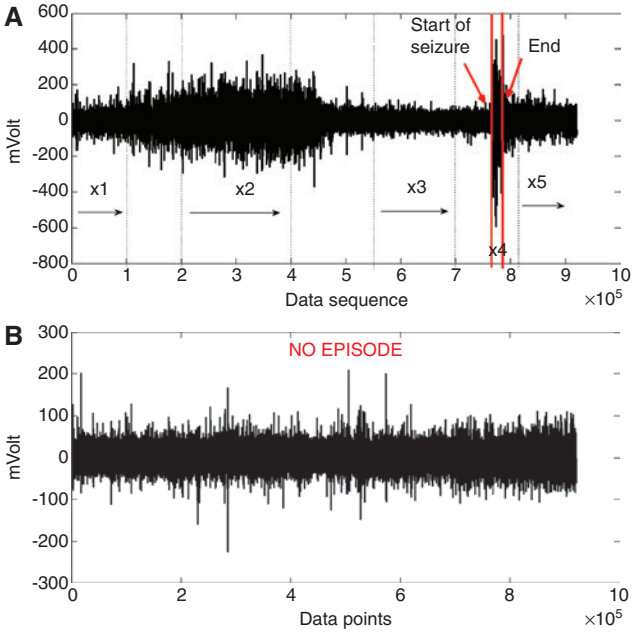

Figure 1: Tsallis q-triplet of two EEG time series concerning epileptic and healthy states.
(A) EEG time series including an epileptic episode. The initiation of the episode and its end is denoted by the red vertical lines. (B) EEG time series of the same patient with no episode.

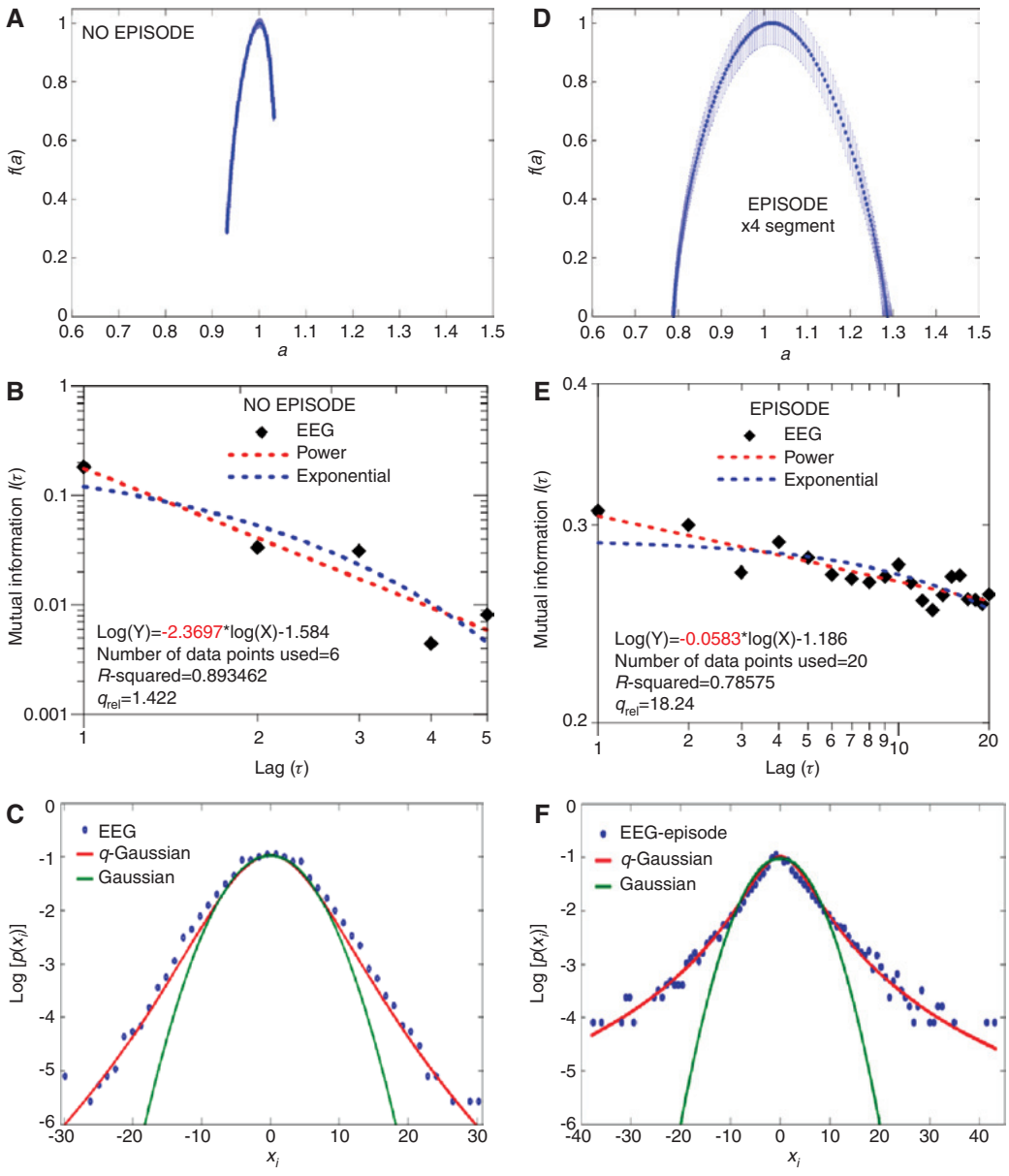

Figure 2: Results concerning the two time series.
(A) The singularity spectra $f(a)$ as a function of singularity strength a for the EEG time series with no episode. (B) Double logarithmic plot of auto-mutual Information $I(\tau)$ vs. τ. for the EEG time series with no episode. (C) $\log(p(x_i))$ vs. x_i graph for the EEG time series with no episode. (D) The singularity spectra $f(a)$ as a function of singularity strength a for the EEG episode time series. (E) Double logarithmic plot of auto-mutual information $I(\tau)$ vs. τ. for the EEG episode time series. (F) $\log(p(x_i))$ vs. x_i graph for the EEG episode time series.

In particular, in Figure 2A,D we show the results concerning the estimation of singularity spectrum $f(a)$ along with error bars and consequently for the Tsallis q_{sen} index (as described in paragraph 2.1.1.1). As it is shown, both time series have multifractal characteristics, but the EEG episode time series clearly exhibits a far richer and wider multifractal spectrum than the one with no episode, indicating that the former time series is more erratic and intermittent than the latter and is a result of an intense complex self-similar behavior which manifests in many scales. This is clearly depicted by the estimation of the Tsallis q_{sen} index. According to [21], when q_{sen} is estimated below unity through Eq. (3), then a power law behavior (instead of exponential) is valid for sensitivity of initial conditions, namely $\xi \propto t^{\lambda_{q_{sen}}} = t^{1/(1-q_{sen})} (t \to \infty)$. The results concerning the Tsallis q_{sen} index for the two time series showed that the Tsallis q_{sen} is below unity for both time series, $q_{senEPISODE} = -1.038 \pm 0.00155 > q_{senNOEPISODE} = -6.976 \pm 0.128$. Therefore, according to the values of the Tsallis q_{sen} and using the q-generalized Pesin-like identity ($K_{q_{ent}} \equiv \lambda_{q_{sen}}$ with $q_{ent} = q_{sen}$) the time series connected with a greater loss of information

in phase space is the EEG episode time series, since $\xi_{EPISODE}=t^{0.49}>\xi_{NOEPISODE}=t^{0.1253}$, and with a greater rate of entropy production since $K_{EPISODE}>K_{NOEPISODE}$.

In Figure 2B,E we present results concerning the Tsallis q_{rel} index. In particular, in these figures we present the best $\log I(\tau)$ vs. $\log(\tau)$ fitting of the auto-mutual information function for the two time series. With the red-dashed lines we emphasize the power law fitting, while with the blue-dashed line we show the exponential fitting. For a classical BG-process the mutual information should decay in an exponential fashion. However, for the two time series we do not find any such behavior. In particular, the mutual information decays in a q-exponential manner (power law) for lags τ=1–5 for the time series with no episode and lags τ=3–20 for the EEG episode time series. The coefficient of determination for the power law fitting (R-squared) was found to be $R^2>0.89$ for the EEG time series with no episode and $R^2>0.78$ for the EEG episode time series, while for the exponential fitting the corresponding values were $R^2<0.81$ and $R^2<0.65$, respectively. Thus, we can use the slope b of the power law fitting to estimate q_{rel} index, as described in Section 2.1.1.2. The results showed that the q_{rel} index was found to be $q_{rel}>1$ for all cases, namely $q_{relNOEPISODE}=1.422\pm0.05<q_{relEPISODE}=18.24\pm2.47$, indicating similar q_{rel}-exponential decay relaxation times to meta-equilibrium non-extensive stationary states for the time series, but also significant differences since the Tsallis q_{rel} index is much higher for the EEG episode time series.

Finally, we also estimated the Tsallis q_{stat} index for the two time series. In Figure 2C,F, we present the results concerning Tsallis q-Gaussians depicted by the solid red line in a $\log[p(x_i)]$ vs. x_i graph, where the difference between the q-Gaussian and the Gaussian PDF (green line) in long tails is clearly visible. The open blue circles correspond to the EEG time series. The Tsallis q-Gaussians correspond to the best linear correlation between $\ln_q[p(x_i)]$ and $(x)_i^2$ (not shown here) and the Tsallis q_{stat} index was found to be above unity in both cases and particularly $q_{statNOEPISODE}=1.192\pm0.023<q_{statEPISODE}=1.4\pm0.07$. The corresponding cc are: 0.95±0.034 and 0.935±0.023, respectively. The high value of the Tsallis q_{stat} index corresponding to the EEG episode time series indicates that the presence of long-range interactions, characterized by non-Gaussian (q-Gaussian) distributions, are much more significant in seizure dynamics than in dynamics with no episode.

In addition, we estimated the Tsallis q-triplet indices for five segments of the time series including the episode shown in Figure 1A, in order to unravel possible variations of Tsallis indices connected to significant shifts of the underlying dynamics. Figure 3 shows the results of the Tsallis q-triplet estimation along with the error bars concerning the five segments of Figure 1A. As shown in Figure 3A for Tsallis q_{stat}, Figure 3B for Tsallis q_{sen} and Figure 3C for Tsallis q_{rel}, Tsallis q-triplet indices of the x4 segment (epileptic episode) attain much higher values compared to the corresponding of the other segments, indicating a shift in the underlying dynamics and a strengthening in the non-extensive character of the system. In addition, Tsallis q_{stat} and q_{sen} indices show a gradual increase in their values as the time of epileptic episode approaches. This result could be related to the significant changes of the brain dynamics from healthy to epileptic states.

Overall, the results showed that the brain system in epileptic dynamics is in an off-equilibrium stationary state whose physics is properly described by the q-statistical mechanics since the Tsallis q-triplet indices adopted the values: $\{q_{sen}; q_{rel}, q_{stat}\}=\{-1.038; 4.34; 1.41\}$, verifying a possible general scheme, $q_{sen}<1<q_{stat}<q_{rel}$ as noted in [13]. The results also indicate that the estimation of the Tsallis q-indices could be used as possible biomarkers, along with others, for improving prediction of epileptic seizures, since the Tsallis indices capture efficiently the difference between healthy and epileptic dynamics (the Tsallis q-triplet is much smaller for no episode dynamics, compared to the epileptic dynamics).

3.2 Gait dynamics in degenerative diseases

In this section, gait dynamics are analyzed in terms of Tsallis statistics. Gait dynamics are related to neurodegenerative diseases since the latter often affect gait and mobility. In particular, we estimate the Tsallis q_{stat} index using the methods described previously corresponding to ALS, PD, HD and healthy controls [26, 27].

The time series analyzed are constructed from the records of the Physionet's database (http://physionet.org/physiobank/database/gaitndd/). They are concerned with stride-to-stride measures of footfall contact times and their analysis could help to understand better the pathophysiology and dynamics of the aforementioned diseases. The analyzed time series are shown in Figure 4A–H and correspond to left and right stride intervals (s). As the plots show, the stride intervals are irregular and non-periodic.

In the following, we present four tables with the results concerning Tsallis q-triplet indices estimation for ALS, PD and HD and a healthy control subject.

3.2.1 Amyotrophic lateral sclerosis

For the study of gait dynamics in ALS we chose a female subject of age 40 years, height 1.7 m and weight 61.24 kg.

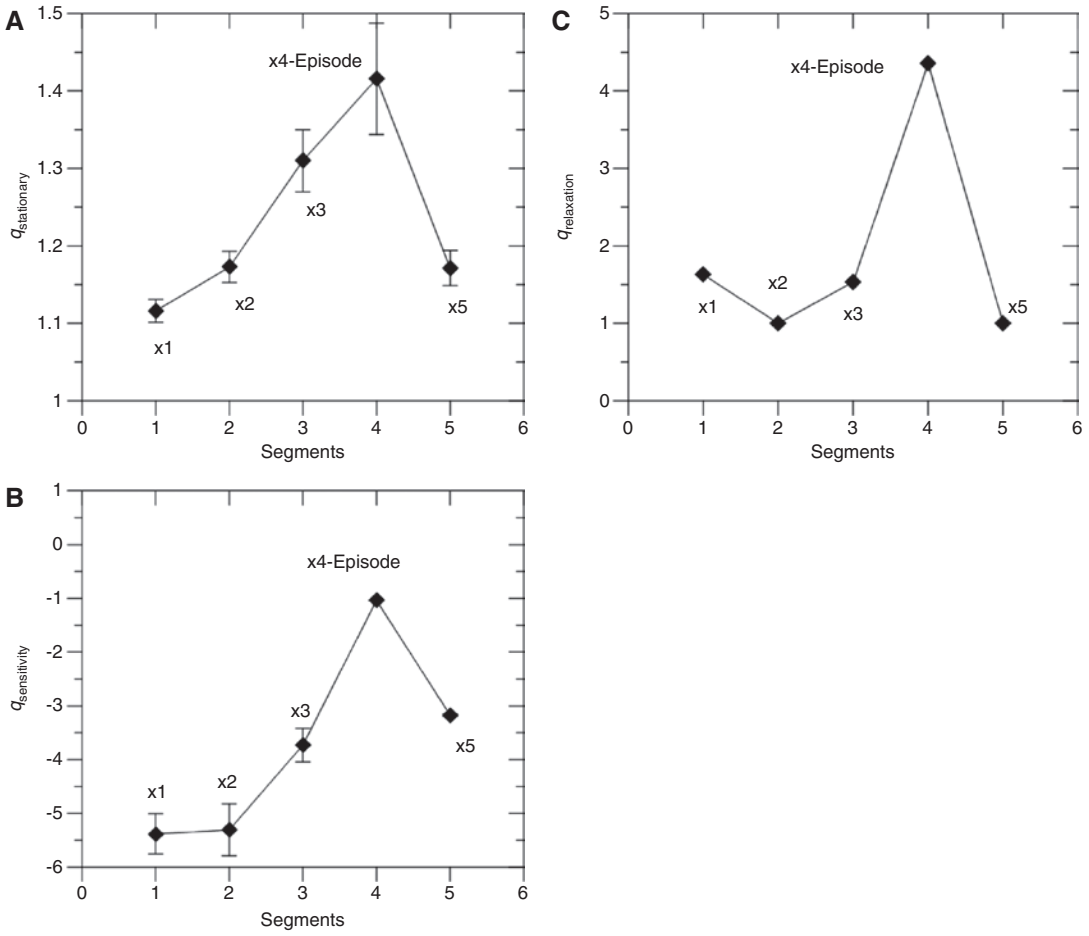

Figure 3: Tsallis indices.
(A) Tsallis q_{stat} index estimated for the five segments of Figure 1A. (B) Tsallis q_{sen} index estimated for the five segments of Figure 1A. (C) Tsallis q_{rel} index estimated for the five segments of Figure 1A.

The time series consisted of 245 stride intervals. The results are presented in Table 1 along with the fitting parameters. In particular, the Tsallis q-triplet was found to be $\{q_{sen}; q_{rel}; q_{stat}\}=\{0.1945; 4.24; 1.22\}$ for left stride intervals and $\{q_{sen}; q_{rel}; q_{stat}\}=\{0.113; 4.16; 1.78\}$ for right stride intervals, respectively. Therefore, in both cases, the indices attained values different from unity denoting non-Gaussian statistics described efficiently by Tsallis non-extensive statistics. In addition, the Tsallis q_{stat} index is higher for right stride intervals indicating a possible asymmetry in the subject's movement and especially more correlated right strides.

3.2.2 Parkinson's disease

For the study of gait dynamics of PD we chose a data set of a male subject of age 77 years, height 2 m and weight 86 kg. The time series consisted of 245 stride intervals. The results are presented in Table 2 along with the fitting parameters. In particular, the Tsallis q-triplet was found to be $\{q_{sen}; q_{rel}; q_{stat}\}=\{0.18; 3.76; 1.6\}$ for left stride intervals and $\{q_{sen}; q_{rel}; q_{stat}\}=\{0.352; 2.32; 1.395\}$ for right stride intervals, respectively. Therefore, in both cases, the indices attained values different from unity, denoting non-Gaussian, which can be described faithfully within Tsallis non-extensive statistics framework. In addition, the Tsallis indices values were different for left and right stride intervals indicating a possible asymmetry in the subject's movement.

3.2.3 Huntington's disease

For the study of Huntington's gait dynamics we chose a data set of a male subject of age 42 years, height 1.86 m and weight 72 kg. The time series consisted of 310 stride intervals. The results are presented in Table 3 along with fitting parameters. In particular, Tsallis q-triplet was found to be $\{q_{sen}; q_{rel}; q_{stat}\}=\{0.613; 2.3; 0.8625\}$ for left stride intervals and $\{q_{sen}; q_{rel}; q_{stat}\}=\{0.226; 3.253; 1.385\}$

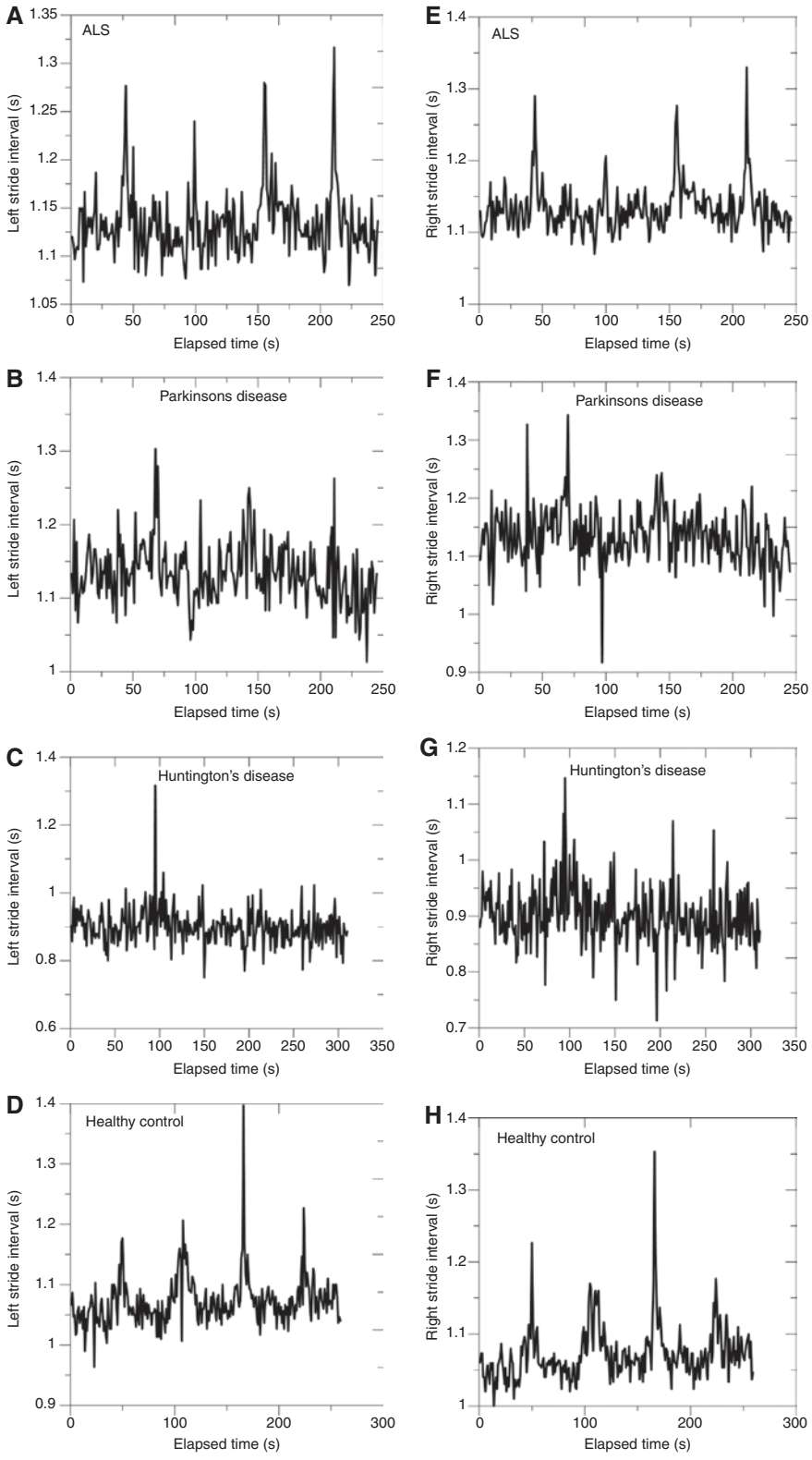

Figure 4: Examples of gait time series.
(A) Left stride intervals for a patient with ALS. (B) Left stride intervals for a patient with Parkinson's disease. (C) Left stride intervals for a patient with Huntington's disease. (D) Left stride intervals for a healthy control subject. (E) Right stride intervals for a patient with ALS. (F) Right stride intervals for a patient with Parkinson's disease. (G) Right stride intervals for a patient with Huntington's disease. (H) Right stride intervals for a healthy control subject.

Table 1: Tsallis q-triplet for stride intervals corresponding to a female subject with amyotrophic lateral sclerosis (ALS).

Stride interval (s)	q_{stat}	q_{sen}	q_{rel}
Left	1.22±0.0606 cc=0.927±0.01	0.1945±0.015	4.24±0.22 R^2=0.92±0.08
Right	1.78±0.23 cc=0.95±0.02	0.113±0.05	4.16±0.6 R^2=0.89±0.05

Table 2: Tsallis q-triplet for stride intervals corresponding to a subject with Parkinson's disease (PD).

Stride interval (s)	q_{stat}	q_{sen}	q_{rel}
Left	1.6±0.12, cc=0.95±0.04	0.182±0.0577	3.7565±0.244 R^2=0.773±0.07
Right	1.395±0.055, cc=0.815±0.015	0.352±0.02	2.32±0.04 R^2=0.738±0.18

Table 3: Tsallis q-triplet for stride intervals corresponding to a subject with Huntington's disease (HD).

Stride interval (s)	q_{stat}	q_{sen}	q_{rel}
Left	0.8625±0.017, cc=0.915±0.01	0.613±0.0106	2.3±0.2 R^2=0.836±0.11
Right	1.385±0.2, cc=0.9586±0.044	0.226±0.013	3.253±0.25 R^2=0.838±0.14

Table 4: Tsallis q-triplet for stride intervals corresponding to a healthy control subject.

Stride interval (s)	q_{stat}	q_{sen}	q_{rel}
Left	2.2±0.37, cc=0.73±0.07	0.487±0.025	3.146±0.6 R^2=0.843±0.08
Right	2.04±0.38, cc=0.79±0.05	0.49±0.01	3.392±0.95 R^2=0.78±0.15

for right stride intervals, respectively. Therefore, in both cases, the indices attained values different from unity denoting non-Gaussian, non-extensive Tsallis statistics. In addition, the Tsallis indices values were significantly different for left and right stride intervals indicating strong asymmetry in the subject's movement resulting in unsteady-jerky gaits. For example, the Tsallis q_{stat} index for the left strides is below unity, while for the right strides it is above unity.

3.2.4 Healthy control

For the study of gait dynamics of a healthy control subject we chose a data set of a female subject of age 57 years, height 1.94 m and weight 95 kg. The time series consisted of 259 stride intervals. The results are presented in Table 4 along with the fitting parameters. In particular, the Tsallis q-triplet was found to be $\{q_{sen}; q_{rel}; q_{stat}\}=\{0.487; 3.146; 2.2\}$ for left stride intervals and $\{q_{sen}; q_{rel}; q_{stat}\}=\{0.49; 3.392; 2.04\}$ for right stride intervals, respectively. Therefore, in both cases, the indices attained values different from unity denoting non-Gaussian, Tsallis non-extensive statistics. In addition, the Tsallis indices values were very similar for left and right stride intervals, indicating strong symmetry in the subject's movement resulting in steady-correlated gaits, as expected from a healthy person.

4 Summary and conclusions

In this paper, we analyzed the statistical features of six time series concerning neurodegenerative disorders. In particular, we studied two EEG time series concerning healthy and epileptic states, as well as time series concerning gait dynamics of ALS, PD and HD and a healthy control. The methodology adopted is based on Tsallis non-extensive statistics and in particular on the Tsallis q-triplet. In particular, we established:

EEG time series

- The strong multifractal character of EEG episode time series compared to the EEG time series which did not include an episode.
- The non-extensive and non-Gaussian character of both EEG time series, based on the estimation of the Tsallis q_{sen} index which was found different from unity in both cases. However, the comparison of the Tsallis q_{sen} index showed that the EEG episode time series is connected with a greater loss of information and entropy production, than the EEG time series with no episode.
- The non-extensive and non-Gaussian character of both EEG time series based on the estimation of Tsallis q_{rel} index, since $q_{rel}>1$, indicating a q_{rel}-exponential decay relaxation of the system to meta-equilibrium non-extensive stationary states. However, the Tsallis q_{rel} index is higher for the EEG episode time series.
- The non-extensive and non-Gaussian (Tsallis q-Gaussian) character of both EEG time series, since the PDFs are efficiently described by Tsallis q-Gaussian distributions characterized by the parameter q_{stat}. In all cases,

the Tsallis index $q_{stat}>1$, indicating super-q-Gaussian statistics, but q_{stat} for EEG episode time series is significantly higher, indicating more correlated dynamics.
- The study of the Tsallis q-triplet concerning the five segments of the EEG time series including the seizure, showed that Tsallis indices corresponding to the epileptic episode attain much higher values compared to the other segments, as well as a gradual increase of the indices (especially of q_{stat} and q_{sen}) as the time of epileptic episode approaches. This result could be related to significant changes (e.g. phase transitions) of the brain dynamics from healthy to epileptic states.

Gait time series
- ALS: The Tsallis q-triplet was found different from unity in all cases indicating non-extensive, non-Gaussian dynamics. However, differences in the Tsallis q_{stat} index concerning left and right stride intervals indicate possible weak asymmetry in the subject's movement, which could be due to weakness, fatigue, loss of balance and coordination of the subject.
- PD: Tsallis q-triplet was found different from unity in all cases indicating non-extensive, non-Gaussian dynamics. However, differences in all Tsallis indices concerning left and right stride intervals indicate an asymmetry in the subject's movement, a result which is in accordance with the Parkinsonian gait dynamics, which is characterized by small shuffling steps and a general slowness of movement.
- HD: The Tsallis q-triplet was found different from unity in all cases indicating non-extensive, non-Gaussian dynamics. A very significant difference was found concerning the Tsallis q_{stat} index. In particular, the Tsallis q_{stat} index for left strides is below unity, while for right strides is above unity. In addition, the other Tsallis indices are also different. These results indicate a strong asymmetry in the subject's movement resulting in from uncoordinated, unsteady-jerky gaits.
- Healthy control: The Tsallis q-triplet was found different from unity in all cases indicating non-extensive, non-Gaussian dynamics. However, all indices were found similar for left and right stride intervals, a result which indicates strong symmetry in the subject's movement resulting in steady-correlated gaits, as expected from a healthy person.

Overall, the results showed that the brain system in epileptic dynamics is in an off-equilibrium stationary state whose physics is properly described by the q-statistical mechanics since the Tsallis q-triplet indices adopted the values: $\{q_{sen}; q_{rel}; q_{stat}\}=\{-1.038; 4.34; 1.41\}$, verifying a possible general scheme, $q_{sen}<1<q_{stat}<q_{rel}$ as noted in [13]. The results also indicate that the estimation of Tsallis q-indices could be used as possible biomarkers, along with others, for improving the prediction of epileptic seizures, since Tsallis indices capture efficiently the difference between healthy and epileptic dynamics (the Tsallis q-triplet is much smaller for no episode dynamics, compared to the epileptic dynamics), as well as possible phase transitions of the brain dynamics as the seizure time approaches. In addition, the results concerning gait dynamics of ALS, PD and HD and healthy control, show that the Tsallis q-triplet is different from unity in all cases considered, thus indicating that the temporal fluctuations in the stride interval are not random but there is hidden information connected with Tsallis q-Gaussians distributions, characterized by the presence of long-range dependence. In addition, differences in Tsallis indices concerning the left and right stride intervals possible, which were more intense in HD (no differences were found in the healthy control subject) represent the subject's gait asymmetry. Therefore the aforementioned results can provide valuable information, indicating different effects of each disease on gait asymmetry and nonlinearity on stride dynamics, changing with each disease providing new insights in disease severity, medication utility and falls in order to improve therapeutic interventions. These results are also in accordance with [8, 28], who found fractal correlations in gait dynamics. Of course, in order to draw safer conclusions more subjects should be examined both for EEGs concerning epilepsy, as well as for gait time series of the aforementioned neurodegenerative diseases.

Finally, the estimation of the Tsallis q-triplet could also be helpful for the discrimination of different types of epileptic seizures and/or provide valuable information concerning EEGs of other neurodegenerative disorders, such as the Alzheimer's disease. Moreover, Tsallis statistics could help to clarify the differences and the similarities between the gait dynamics of the same disease as well as between the diseases, since the temporal fluctuations in the stride interval change with age and disease [12]. In addition, other time series corresponding to sub-phases of the stride (e.g. stance and swing) could be examined.

References

[1] World Health Organization. *Neurological Disorders: Public Health Challenges*, WHO Press: Geneva, Switzerland, 2006.
[2] Tsoutsouras VG, Sirakoulis GC, Pavlos GP, Iliopoulos AC. *Int. J. Bifurcation Chaos* 2012, 22, 1250229.

[3] Acharya RU, Molinari F, Vinitha Sree S, Chattopadhyay S, Ng K-H, Suri JS. *Biomed. Signal Process. Control* 2012, 7, 401–408.
[4] Aziz W, Arif M. *Eur. J. Appl. Physiol.* 2006, 98, 30–40.
[5] Plastino A, Rosso OA. *Europhys. News* 2005, 36, 224–228.
[6] Zeng W, Wang C. *Inform. Sciences* 2015, 317, 246–258.
[7] Walleczek J. *Self-Organized Biological Dynamics and Nonlinear Control*, Cambridge University press: New York, USA, 2000.
[8] Hausdorff JM, Ashkenazy Y, Peng CK, Ivanov PC, Stanley HE, Goldberger AL. *Physica A* 2001, 302, 138–147.
[9] Iasemidis LD, Shiau DS, Sackellares JC, Pardalos PA, Prasad A. *IEEE Trans. Biomed. Eng.* 2004, 51, 493–506.
[10] Goldberger AL, Amaral LAN, Hausdorff JM, Ivanov PCh, Peng K-C, Stanley HE. *Proc. Natl. Acad. Sci. U.S.A.* 2002, 99, 2466–2472.
[11] Stam CJ. *Clin. Neurophys.* 2005, 116, 2266–2301.
[12] Delignières D, Torre K. *J. Appl. Physiol.* 2009, 106, 1272–1279.
[13] Tsallis C. *Introduction to Nonextensive Statistical Mechanics: Approaching A Complex World*, Springer: Berlin, 2009, 1–378.
[14] Capurro A, Diambra L, Lorenzo D, Macadar O, Martin MT, Mostaccio C, Plastino A, Pérez J, Rofman E, Torres ME, Velluti J. *Physica A* 1999, 265, 235–254.
[15] Martin MT, Plastino AR, Plastino A. *Physica A* 2000, 275, 262–271.
[16] Eftaxias K, Minadakis G, Potirakis SM, Balasis G. *Physica A* 2013, 392, 497–509.
[17] Tsallis C. *Physica A* 2004, 340, 1–10.
[18] Pavlos GP, Karakatsanis LP, Iliopoulos AC, Pavlos EG, Xenakis MN, Clark P, Duke J, Monos DS. *Physica A*, 2015, 438, 188–209.
[19] Pavlos GP, Karakatsanis LP, Xenakis MN, Pavlos EG, Iliopoulos AC, Sarafopoulos DV. *Physica A* 2014, 395, 58–95.
[20] Lyra LM, Tsallis C. *Phys. Rev. Lett.* 1998, 80, 53–56.
[21] Tsallis C. *Int. J. Bifurcation Chaos* 2012, 22, 1230030.
[22] Fraser AM, Swinney LH. *Phys. Rev. A* 1986, 33, 1134–1140.
[23] Umarov S, Tsallis C, Steinberg S. *Milan J. Math.* 2008, 76, 307–328.
[24] Goldberger AL, Amaral LAN, Glass L, Hausdorff JM, Ivanov PCh, Mark RG, Mietus JE, Moody GB, Peng C-K, Stanley HE. *Circulation* 2000, 101, e215–e220 [Circulation Electronic Pages; http://circ.ahajournals.org/cgi/content/full/101/23/e215].
[25] Shoeb A. *Application of Machine Learning to Epileptic Seizure Onset Detection and Treatment*, PhD Thesis, Massachusetts Institute of Technology, 2009.
[26] Hausdorff JM, Mitchell SL, Firtion R, Peng CK, Cudkowicz ME, Wei JY, Goldberger AL. *J. Appl. Physiol.* 1997, 82, 262–269.
[27] Hausdorff JM, Lertratanakul A, Cudkowicz ME, Peterson AL, Kaliton D, Goldberger AL. *J. Appl. Physiol.* 2000, 88, 2045–2053.
[28] Hausdorff JM. *Hum. Mov. Sci.* 2007, 26, 555–589.